Available online at www.sciencedirect.com
ScienceDirect
Ceramics International 38S (2012) S319–S322
CERAMICS INTERNATIONAL
www.elsevier.com/locate/ceramint

Fine structural analysis and phase transition behavior for Li-modified $Na_{0.5}K_{0.5}NbO_3$ lead-free piezoelectric ceramics

Ken-ichi Kakimoto *, Tatsuro Hotta, Isao Kagomiya

Department of Materials Science and Engineering, Graduate School of Engineering, Nagoya Institute of Technology, Gokiso-cho, Showa-ku, Nagoya 466-8555, Japan

Available online 4 May 2011

Abstract

The fine crystal structure of $Li_x(Na_{0.5}K_{0.5})_{1-x}NbO_3$ ceramics has been studied by means of Nb-*K* edge extended X-ray absorption fine structure (EXAFS) and X-ray internal strain measurement technique in the vicinity of the compositions showing a polymorphic phase boundary (PPB) between orthorhombic and tetragonal structures. The anisotropic distortion of the NbO_6 octahedral initially occurred when x was increased from 0.050 to 0.053, prior to the completion of the phase transition from orthorhombic to tetragonal symmetry. EXAFS clearly revealed that the bond distance of Nb–O1 with [0 0 1] configuration was increased, and that of Nb–O2 with [1 1 0] configuration was oppositely decreased in the NbO_6 octahedral. In the vicinity of the PPB compositions, the internal strain $\eta_{(0\ 1\ 1)}$ also increased from 4.5×10^{-3} to the maximum value of 12.0×10^{-3} in the narrow x range from 0.040 to 0.055, then decreased to 3.2×10^{-3} at $x = 0.06$. On the other hand, the $\eta_{(1\ 0\ 0)}$ increases from 1.5×10^{-3} to the maximum value of 2.9×10^{-3} in the next narrow x range from 0.055 to 0.060. The variation of $\eta_{(1\ 0\ 0)}$ differed in Li dependence from that of $\eta_{(0\ 1\ 1)}$, which indicates that a large anisotropic strain remains in the crystal lattice in the PPB compositions.

Keywords: B. X-ray method; C. Piezoelectric properties; D. Niobates; Phase transition

1. Introduction

Perovskite solid solutions based on sodium potassium niobate ($Na_xK_{1-x}NbO_3$, abbreviated as NKN-100x) have been extensively studied as a promising lead-free candidate for replacing $Pb(Zr_xTi_{1-x})O_3$ (PZT) ceramics [1–5]. In particular, the compositions around NKN-50 have received much attention owing to their high piezoelectric constant d_{33} of ~160 pC/N and enhanced radial electromechanical coupling coefficients (k_p) of ~0.45 [6,7]. NKN-50 ceramics cause a sequential phase transition similar to $BaTiO_3$ with elevated temperature: i.e., ~210 °C for orthorhombic to tetragonal ($T_{o\text{-}t}$) and ~420 °C for tetragonal–cubic (T_c) phase transitions [8].

It is now generally accepted that Li substitution for NKN-50 cell, being $Li_x(Na_{0.5}K_{0.5})_{1-x}NbO_3$ (abbreviated as LNKN-100x), can decrease $T_{o\text{-}t}$ from 210 °C to near the room temperature without lowering of T_c, which is rather increased from 420 °C to higher temperature toward 500 °C [2]. We also reported that the highest piezoelectric constant d_{33} of 235 pC/N could be successfully obtained at room temperature for LNKN-6 ceramics in which Li content was controlled to be 6 mol% ($x = 0.06$). Such excellent piezoelectric property seems to be associated with the fact that $T_{o\text{-}t}$ is shifted in the vicinity of room temperature where a polymorphic phase boundary (PPB) between orthorhombic and tetragonal structures can enhance the electrical property of the ceramics owing to the coexistence of their multiple polarization vectors.

Additionally, Li substitution should also form local stresses inside NKN-50 unit cell, since the small ionic diameter of Li^+ is not enough to form a perovskite structure as an A-site ion solely with NbO_5^-, which may contribute to irreversible structure change in NKN-50 unit cell. Sun et al. [9] found, from X-ray Rietveld analysis, that the atomic position of A-site ions of LNKN-6 shifted in the negative [0 0 1] direction against the coordinated oxygen atoms and enhanced the spontaneous polarization, compared to NKN-50. In our previous study [10], Raman scattering technique also recognized that NbO_6^- octahedral unit was locally distorted in LNKN unit cell by increasing Li content.

* Corresponding author. Tel.: +81 52 735 7734; fax: +81 52 735 7734.
E-mail address: kakimoto.kenichi@nitech.ac.jp (K.-i. Kakimoto).

0272-8842/$36.00
doi:10.1016/j.ceramint.2011.04.110

However, it is still unclear that the fine structure and its variation in the vicinity of the PPB compositions for LNKN ceramics. In this study, therefore, the extended X-ray absorption fine structure (EXAFS) analysis using synchrotron radiation was carried out together with X-ray internal strain measurement in order to give additional understandings for the determination of the true structure.

2. Experimental procedures

A nominal composition of $Li_x(Na_{0.5}K_{0.5})_{1-x}NbO_3$ (LNKN-100x), where x was varied from 0 to 0.08, was prepared using Li_2CO_3 powder of 99% purity, and Na_2CO_3, K_2CO_3 and Nb_2O_5 powders of 99.9% purity. All of the powders were mixed to make appropriate compositions, then ball-milled in ethanol medium for 24 h. A dried sample was calcined at 850 °C for 10 h, followed by crushing and adding 3 wt% of poly(vinyl alcohol) as a binder. The granulated powders were uniaxially pressed into disks of 12 mm in diameter and 1 mm in height, followed by cold isostatic pressing under 200 MPa. The disks were sintered in air at selected temperatures, depending on the value of x, in the range between 1076 and 1100 °C for 2 h to obtain dense ceramics with 95% of the theoretical density or more.

The EXAFS measurements of the pulverized samples at near Nb-K edge were performed at room temperature in N_2–Ar-gas-mixture filled ionization chambers at the synchrotron radiation beam line BL-7C in the Photon Factory of the High Energy Accelerator Research Organization (PF-KEK), Tsukuba, Japan. The X-ray absorption spectra were monitored in the energy range from 18.7 to 19.5 keV. The averaged EXAFS data were analyzed by using REX2000 (Rigaku, Japan) and FEFF (Univ. Washington, USA) [11] programs. The EXAFS oscillation, $|(k)$, was extracted from the spectrum using the Victreen function and the cubic sprain technique. The Fourier transforms (FT) of $k^3|(k)$ yielded the radial distribution functions (RDFs).

The internal strain η was calculated from the following equation [12]:

$$\beta \cos\theta = \frac{\lambda}{d} + 2\eta \sin\theta \quad (1)$$

where β is the full-width at half-maximum (FWHM) of the X-ray diffraction peaks, λ is the wave length of X-ray, and d is the size of crystalline. Since the grain size (d) of the ceramics is sufficiently larger than λ (CuKα: 1.54056 Å), Eq. (1) can be simplified by

$$\beta = 2\eta \tan\theta \quad (2)$$

The raw X-ray diffraction data were collected by the step scanning technique in a PANalytical X'pert PRO–MRD system, Netherlands. Their angle θ and β were refined by using a PRO-FIT program, QuantumSoft, Switzerland. Rietveld analysis was carried out by a Rietan-2000 program [13].

3. Results and discussion

The local NbO_6 structure of LNKN ceramics was characterized by EXAFS experiment. Fig. 1 shows the near Nb-K edge EXAFS oscillation corresponding to LNKN-6 for instance. The k^3-weighed signals of the Nb core atoms at the range of 3–12 Å^{-1} in k space showed strong absorbance caused by the backscattering of Nb-surrounding atoms. After elimination of the backgrounds from the curve, the Fourier transformation of the k-weighed $k^3|(k)$ signals was carried out. To deduce the structural parameters of NbO_6, the FEFF program calculated the backscattering interference paths in the k space.

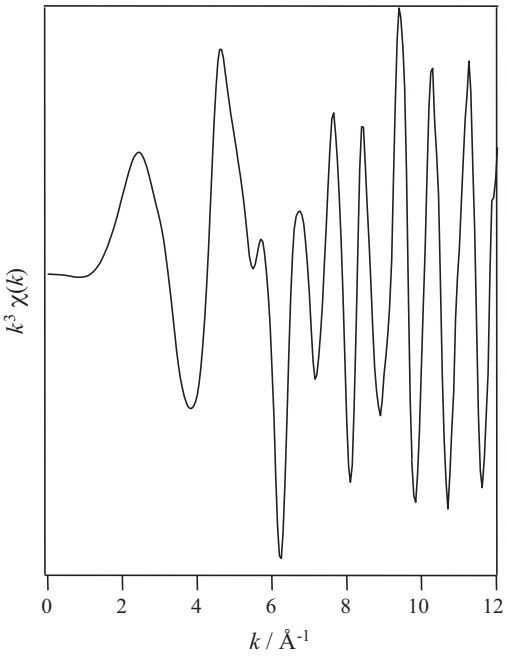

Fig. 1. k^3-weighted EXAFS signal of the Nb-K-edge in k space for LNKN-6.

The derived RDFs around Nb-K absorption edge for LNKN ceramics in the vicinity of the PPB compositions are shown in Fig. 2, together with simulated $LiNbO_3$ (ICSD-28297), $NaNbO_3$ (ICSD-97669) and $KNbO_3$ (ICSD-39869)

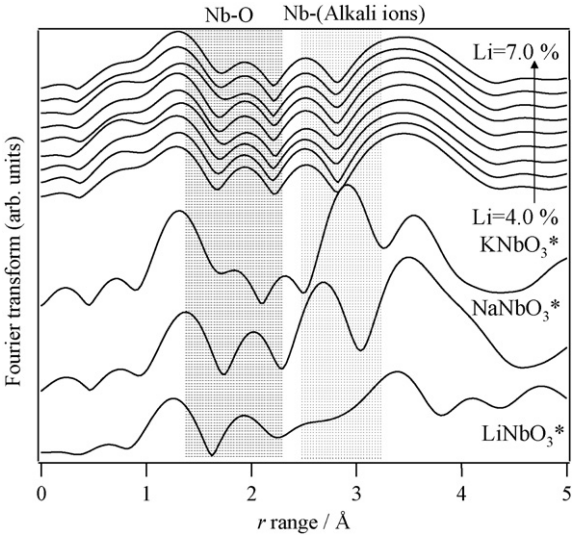

Fig. 2. Radial distribution functions (RDFs) around Nb-K absorption edge for LNKN ceramics and the FEFF-simulated niobates profiles.

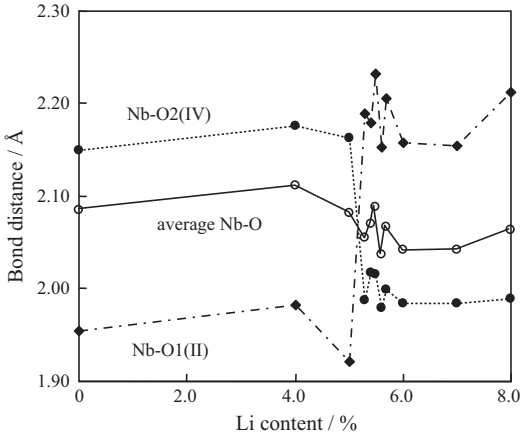

Fig. 3. Correlation of the Nb–O bond distances and Li content. Nb–O1(II) and Nb–O2(IV) corresponds to the orthogonal configurations of two [0 0 1] and four [1 1 0] directions of NbO_6 octahedral, respectively.

profiles. The *R*-factors of the refinement were all bellow 0.003. All LNKN samples exhibited separated peaks indicating the existence of different Nb–O distances in the *r* range up to 3 Å. The recorded profiles appeared as a good superposition of the three simulation results of the niobates because of their solid solutions, and the peaks located at around 1.5 and 2.8 Å represent the nearest neighbor Nb–O and Nb-(alkali ions), respectively. The appearance of new peak by increase of the Li concentration (x) was not recognized in this analysis.

Fig. 3 compares the two kinds of Nb–O bond distances and their average for LNKN ceramics. In this calculation, the two different sites of O atom (O1 and O2) were assumed to fit the EXAFS parameters. The Nb–O1(II) and Nb–O2(IV) corresponds to the orthogonal configurations of two [0 0 1] and four [1 1 0] directions of NbO_6 octahedral, respectively. According to the average bond distance, the size of NbO_6 apparently decreases from $x = 0.04$ to 0.06. In contrast, the bond distance of Nb–O1(II) increases from 1.92 to 2.19 Å and that of Nb–O2(IV) decreases from 2.16 to 1.98 Å, when x increases from 0.050 to 0.053. As a result, the oxygen atoms would be attracted in the [0 0 1] direction toward Alkali ions, and thus the Nb–O1(II) bond distance would increase. This seems to be well correlated with the fact that dielectric constant, i.e., spontaneous polarization, at room temperature starts to increase abruptly in the LNKN ceramics at $x = 0.053$ and higher.

The XRD patterns measured in the vicinity of the PPB compositions for LNKN ceramics are presented in Fig. 4. It can be clearly seen that the peak of (1 0 0) initially shifts to higher angle then goes back to lower angle with increase of Li content. The bending point occurs around at LNKN-5.5. The FWHM also differs in the (0 1 1)/(1 0 0), (0 2 2)/(2 0 0) and (0 3 3)/(3 0 0) planes, indicating that a large anisotropic strain remains in the crystal lattice. Next, internal strain η values were calculated based on Eq. (2), and the result is shown in Fig. 5. In the vicinity of the PPB compositions, the $\eta_{(0\,1\,1)}$ increased from 4.5×10^{-3} to the maximum value of 12.0×10^{-3} in the narrow x range from 0.040 to 0.055, then decreased to 3.2×10^{-3} at $x = 0.06$. On the other hand, the $\eta_{(1\,0\,0)}$ increases from 1.5×10^{-3} to the maximum value of 2.9×10^{-3} in the next narrow x range from 0.055 to 0.060. Thus, the $\eta_{(1\,0\,0)}$ shows a slight delay in its variation toward its maximized value, compared with $\eta_{(0\,1\,1)}$. It can be therefore speculated that the crystal structure change caused by increasing Li substitution for NKN-50 cell would initiate around the (0 1 1) plane of orthorhombic *Bmm2*, then spread to the (1 0 0) plane, and finish its phase transition to tetragonal *P4mm* finally. The EXAFS result (Fig. 3) also confirmed that Nb–O1(II) and Nb–O2(IV) exchanged their bond distances when the orthorhombic–tetragonal phase transition was finished.

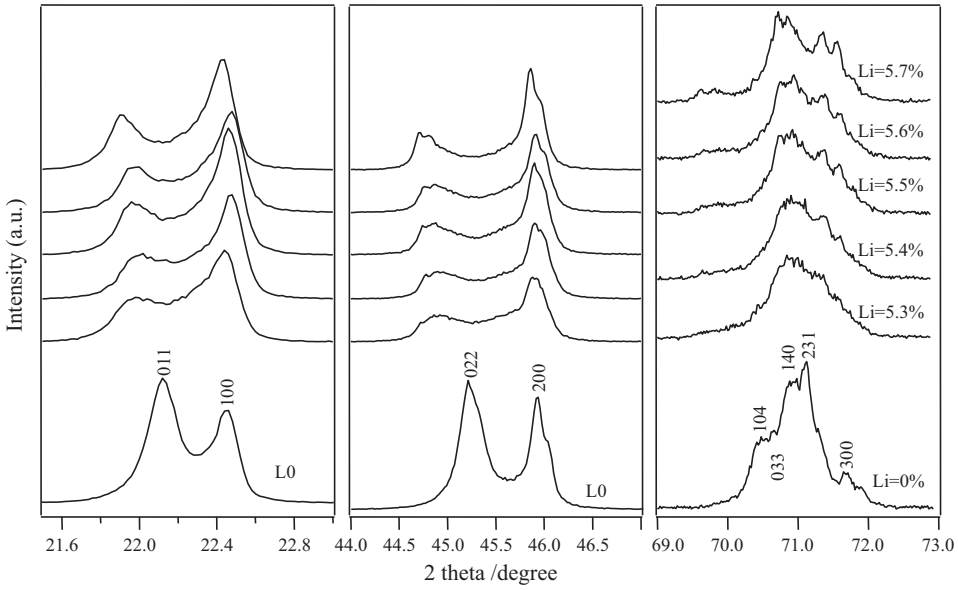

Fig. 4. XRD patterns measured for LNKN ceramics.

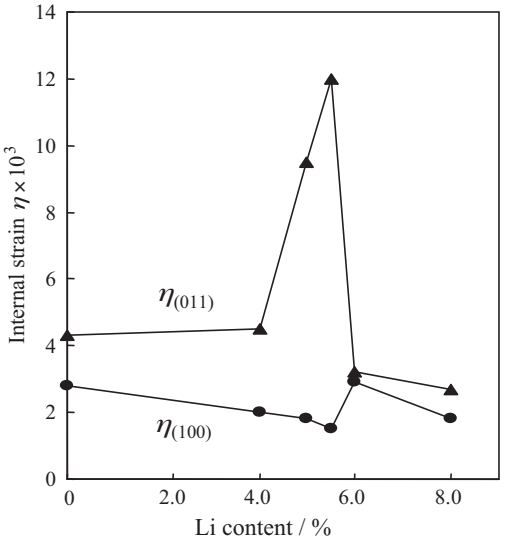

Fig. 5. Variation of internal strain $\eta_{(1\ 0\ 0)}$ and $\eta_{(0\ 1\ 1)}$ as a function of Li content.

4. Conclusions

The local NbO_6 structure of LNKN ceramics in the vicinity of the PPB compositions was investigated by means of EXAFS and X-ray internal strain measurement technique. It was newly found that Li substitution for NKN-50 cell resulted in the anisotropic distortion of the NbO_6 octahedral prior to the completion of the phase transition from orthorhombic to tetragonal symmetry. In this situation, the coordinated oxygen atoms would be attracted in the [0 0 1] direction toward Alkali ions. Thus, it is possible to consider that the accumulated anisotropic distortion in the structure of LNKN-5.5 and LNKN-6 promotes a preferential Nb off-centre and becomes an origin for the enhancement of their large spontaneous polarization and excellent piezoelectric properties.

Acknowledgements

This research was supported by a Grant-in-Aid for Scientific Research B, (No. 21360323) and by the Industrial Technology Research Grant Program in 2007 from the New Energy and Industrial Technology Development Organization (NEDO) of Japan.

References

[1] Y. Guo, K. Kakimoto, H. Ohsato, Structural and electrical properties of lead-free $(Na_{0.5}K_{0.5})NbO_3$–$BaTiO_3$ ceramics, Japanese Journal of Applied Physics 43 (2004) 6662–6666.
[2] Y. Guo, K. Kakimoto, H. Ohsato, Phase transitional behavior and piezoelectric properties of $(Na_{0.5}K_{0.5})NbO_3$–$LiNbO_3$ ceramics, Applied Physics Letter 85 (2004) 4121–4123.
[3] Y. Saito, H. Takao, T. Tani, T. Nonoyama, K. Takatori, T. Homma, T. Nagaya, M. Nakamura, Lead-free piezoelectric ceramics, Nature 432 (2004) 84–87.
[4] M. Matsubara, T. Yamaguchi, K. Kikuta, S. Hirano, Sinter ability and piezoelectric properties of $(K,Na)NbO_3$ ceramics with novel sintering aid, Japanese Journal of Applied Physics 43 (2004) 7159–7163.
[5] R. Wang, H. Bando, T. Katsumata, Y. Inaguma, H. Taniguchi, M. Itoh, Tuning the orthorhombic-rhombohedral phase transition temperature in sodium potassium niobate by incorporating barium zirconate, Physica Status Solidi–Rapid Research Letters 3 (2009) 142.
[6] L. Egerton, D.M. Dillon, Piezoelectric and dielectric properties of ceramics in the system potassium-sodium niobate, Journal of the American Ceramic Society 42 (1959) 438–442.
[7] R.E. Jaeger, L. Egerton, Hot pressing of potassium-sodium niobates, Journal of the American Ceramic Society 45 (1962) 209–213.
[8] G. Shirane, R. Newnham, R. Pepinsky, Dielectric properties and phase transitions of $NaNbO_3$ and $(Na,K)NbO_3$, Physical Review 96 (1954) 581–588.
[9] X. Sun, J. Deng, J. Chen, C. Sun, X. Xing, Effects of Li substitution on the structure and ferroelectricity of $(Na,K)NbO_3$, Journal of the American Ceramic Society 92 (2009) 3033–3036.
[10] K. Kakimoto, K. Akao, Y. Guo, H. Ohsato, Raman scattering study of piezoelectric $(Na_{0.5}K_{0.5})NbO_3$–$LiNbO_3$ ceramics, Japanese Journal of Applied Physics 44 (2005) 7064–7067.
[11] A.L. Ankudinov, J.J. Rehr, Relativistic calculations of spin-dependent X-ray-absorption spectra, Physical Review B56 (1997) R1712–R1715.
[12] A.R. Stokes, A.J.C. Wilson, The diffraction of X rays by distorted crystal aggregates – I, Proceedings of the Physical Society 56 (1944) 174–181.
[13] F. Izumi, T. Ikeda, A rietveld-analysis program RIETAN-98 and its applications to zeolites, Materials Science Forum 198–203 (2000) 321–324.